Manuscript prepared for Biogeosciences
with version 3.0 of the LaTeX class copernicus.cls.
Date: 21 December 2009

Carbon fixation prediction during a bloom of *Emiliania huxleyi* is highly sensitive to the assumed regulation mechanism

Olivier Bernard [1,2], **Antoine Sciandra** [2], **and Sophie Rabouille** [2]

[1]COMORE-INRIA, BP93, 06902 Sophia-Antipolis Cedex, France
[2]LOV, UMR 7093, Station Zoologique, B.P. 28 06234, Villefranche-sur-mer, France

Abstract.

Large scale precipitation of calcium carbonate in the oceans by coccolithophorids plays an important role in carbon sequestration. However, how increased atmospheric CO_2 concentration may affect both calcification and photosynthesis in coccolithophorids is still subject to debate (Riebesell et al., 2008; Iglesias-Rodriguez et al., 2008a). Indeed recent experiments revealed conflicting conclusions, where the associated fluxes were either slowed down or, on the contrary, increased. Bernard et al. (2008) developped several competitive models to account for various scenarii of calcification and photosynthesis regulation in nitrogen limited chemostat cultures of *Emiliania huxleyi*, based on different hypotheses on the regulation mechanism. These models consider that either carbon dioxide, bicarbonate or carbonate is the regulating factor. Here we embedded these biological models into a simple mixed layer model in order to simulate a large bloom of *Emiliania huxleyi*. We also added another biological model relying on the assumption that calcite saturation state (Ω) acts as a regulating factor. From the predicted production of organic carbon, we used current export models to assess the corresponding organic and inorganic carbon exports during the first phase of the bloom. In the decay phase of the bloom, we assumed that a large fraction of the coccolithophorids was predated and finally exported. The models were calibrated to predict the same carbon fixation rate in nowadays pCO_2, and yet, they turned out to respond differently to an increase in CO_2 concentration. It results that models assuming a regulation by CO_3^{2-} or Ω predict much higher carbon fluxes. Models responded differently to a doubled pCO_2 , with those controlled by CO_2 or HCO_3^- leading to increased carbon fluxes. Most importantly, the variability between the different models proved to be in the same order of magnitude as the response to pCO_2 increase. The uncertainty on both the parameter values and the underlying mechanisms that regulate carbon acquisition therefore generate predictions ranges in the same order as an effect of pCO_2 shift, making hasardous any quantitative prediction in a high CO_2 ocean.

Correspondence to: Olivier Bernard, Email: olivier.bernard@inria.fr

1 Introduction

Coccolithophorids play an important role in CO_2 trapping (Frankignoulle et al., 1994), since they transform dissolved inorganic carbon (DIC) into respectively particulate organic and inorganic matter which, being denser than seawater, sink towards the ocean floor.

$$6CO_2 + 12H_2O \longrightarrow C_6H_{12}O_6 + 6O_2 + 6H_20 \quad (1)$$

$$Ca^{2+} + 2HCO_3^- \longrightarrow CaCO_3 + CO_2 + H_2O \quad (2)$$

Such export of both particulate organic carbon (POC) (equation (1)) and particulate inorganic carbon (PIC) (equation (2)), operated by the biological pump from the surface ocean layers, constitutes a carbon sink to the deep ocean on a geological scale (Klepper et al., 1994; Falkowski, 1997).

Coccoliths formation thus accounts for nearly 70% of the biogenic carbonate precipitation in the oceans (Houghton et al., 1996). Yet, such structures are relatively sensitive to pH and tend to dissolve when the water becomes too acidic. It is expected that a doubling in partial pressure of atmospheric CO_2 (pCO_2) will have direct consequences on the ability of these organisms to maintain their growth rate (Riebesell et al., 2000; Sciandra et al., 2003). As a corollary, acidification of the oceans due to increase in atmospheric pCO_2 (Orr et al., 2005) could jeopardize their role as a CO_2 pump.

Hence, how coccolithophorids may respond to shifts in global pCO_2 is a critical question to be addressed. However,

in contrast with the well known chemical phenomena driving the coccoliths dissolution, the effects of pCO_2 changes, whether on photosynthesis or on calcification, are still subject to intense debate (Paasche, 2002; Berry et al., 2002; Riebesell et al., 2008; Iglesias-Rodriguez et al., 2008a). Contradictory observations were made in batch experiments, where doubling pCO_2 either led to a decrease (Riebesell et al., 2000) or an increase (Iglesias-Rodriguez et al., 2008b) in calcification in *Emiliana huxleyi* while photosynthesis was enhanced. Nitrogen limited continuous culture experiments in chemostats supported the hypothesis that both photosynthesis and calcification decrease (Sciandra et al., 2003), whereas photosynthesis was increased in a study with non calcifying strain (Leonardos and Geider, 2005).

Experimental developments on the functional relationship between calcification and photosynthesis have long exhibited contradictory results (see the review by Paasche (2002)). Whether and how photosynthesis is coupled to calcification partly remains a mystery (Berry et al., 2002), which, when unravelled, will shed light on the possible facilitation of photosynthesis by calcification. In particular, the kind of transport (active vs. passive) and the C substrates (CO_2 vs. HCO_3^-) implied in the uptake of DIC are still subject to debate. But recent work on the topic firmly concludes that the process of photosynthesis is not related to the efficiency of calcification (Leonardos et al., 2009; Trimborn et al., 2007b)

Considering the chemical equations for photosynthesis (1) and calcification (2), a classical Michaelis-Menten based kinetics for growth could be proposed, involving respectively CO_2 and HCO_3^-. However, such representation follows the dogmatic assumption that photosynthesis is regulated by the CO_2 concentration only, and calcification is regulated by HCO_3^- only. Yet, Riebesell et al. (2000) and Sciandra et al. (2003) indirectly demonstrated that HCO_3^- could not regulate calcification: their experiments showed that an increase in HCO_3^- led to a decrease in the calcification rate. These contradictory experimental results spurred Bernard et al. (2008) to propose and analyse different biological models derived from different assumptions as for the inorganic carbon species regulating calcification and photosynthesis, taken among CO_2 , HCO_3^- and CO_3^{2-}. In the case of assumed, coupled photosynthesis and calcification, 3 models were obtained, while 6 models were designed when these processes were considered as significantly uncoupled. Model analyses showed that only the models where carbonate ion regulates calcification could reproduce the decrease in calcification rate after a pCO_2 doubling, hence refuting the general assumption of a regulation by HCO_3^- (Bernard et al., 2008). Indeed, CO_3^{2-} is the only species whose concentration decreases when pCO_2 increases (for a constant alkalinity). This hypothesis is corroborated by Merico et al. (2006) who suggest that the condition of high CO_3^{2-} can be considered as a crucial ecological factor for the success of *E. huxleyi*. Nevertheless, this hypothesis lacks clarification and support from a biological point of view. As stated by Riebesell (2004), carbonate saturation state may exert a stronger control on calcification than any of the other possible candidates, e.g. pH, CO_2 , or CO_3^{2-} concentrations. Therefore, we considered that calcite saturation state Ω might also drive the calcification rate, and we introduced a new model, with Ω acting as a regulating factor. The underlying phytoplankton growth model, based on the representation of a cell quota, is a Droop-like model (Droop, 1968; Burmaster, 1979; Droop, 1983) in which we added the dependence to both inorganic carbon and light.

Our goal was to point out how the generic model of (Bernard et al., 2008), successively run with the different regulating factors, predicts significantly different amounts and fluxes of carbon. We simulated the typical situation of an *Emiliania huxleyi* late-Spring bloom, following a diatom bloom which depleted the inorganic carbon stock (Riebesell et al., 1993). The four versions of the model only differ by their assumption on the factor regulating the inorganic carbon uptake of photosynthesis and calcification. In this simplified model, we assume that all the chemical and biological concentrations are homogeneous in the mixed layer. The main idea developed throughout this paper is that some transient phenomena can lead to paradoxical effects on the predicted carbon fluxes. We stress that, depending on the supposed regulating factor, the exported carbon can vary twofold. Results also reveal that the variability of the fluxes, both due to the assumed regulating factor and to parameter uncertainty, is higher than the influence of a pCO_2 increase.

In the following section, we present the biological model of photosynthesis and calcification and describe its variants, according to the chemical species regulating the inorganic carbon compartment. We then recall classical modelling theories of the carbonate system dynamics in seawater. The hydrodynamical structure of the water column, in the considered typical situation, is exposed in section 2. Section 3 is devoted to Monte Carlo model simulations under two environmental conditions, represented by the current pCO_2 and that expected in the end of the 21^{st} century, after a pCO_2 doubling. The results are then discussed in section 5.

2 Modelling a bloom of *E. huxleyi* in a mixed layer

2.1 Growth in conditions of nitrogen limitation: extension of the Bernard et al. (2008) modelling framework

In this section we briefly recall the fundamentals of the modelling framework developed in Bernard et al. (2008) for the biological kinetics. In the present work, these biological models are improved and further included in a simple physical framework representing a mixed layer. The principle of the model development is to account for the process uncertainty, and thus decline a modelling framework into various, structurally identical models to test alternative hypotheses.

	Meaning	Unit
D	Dissolved inorganic carbon (DIC)	$mmol.L^{-1}$
N	Particulate nitrogen (PN)	$mmol.L^{-1}$
Q	Internal nitrogen quota	$mmolN.(mmolC)^{-1}$
X	Particulate organic carbon (POC)	$mmol.L^{-1}$
C	Coccoliths concentration (PIC)	$mmol.L^{-1}$
S_1	Nitrate concentration	$mmol.L^{-1}$
S_2	Calcium concentration	$mmol.L^{-1}$
Ω	Calcite saturation state	-
F^1_{POC}	POC flux during growth phase	$mmolC.day^{-1}.m^{-2}$
F^1_{PIC}	PIC flux during growth phase	$mmolC.day^{-1}.m^{-2}$
F^2_{POC}	POC flux during decay phase	$mmolC.day^{-1}.m^{-2}$
F^2_{PIC}	PIC flux during decay phase	$mmolC.day^{-1}.m^{-2}$

Table 1. Definition of variables and fluxes for the four considered models.

Uptake of inorganic nitrogen (nitrate, denoted S_1 ($mmol.L^{-1}$)) by the coccolithophorid biomass (whose particulate nitrogen concentration is denoted N ($mmol.L^{-1}$)), is represented by the following mass flow, where $\rho(S_1)$ is the nitrate absorption rate:

$$S_1 \xrightarrow{\rho(S_1)X} N \tag{3}$$

Generally, nitrate uptake is assumed to depend on external nitrate concentration NO_3, following a Michaelis-Menten type equation (Dugdale, 1967):

$$\rho(S_1) = \rho_m S_1/(S_1 + k_N) \tag{4}$$

where ρ_m and k_N are the maximum uptake rate and the half-saturation constant, respectively.

The flux of inorganic carbon into organic biomass X ($mmolC.L^{-1}$) and coccoliths C ($mmolC.L^{-1}$) is associated to a flux of calcium (Ca^{2+}, denoted S_2 ($mmol.L^{-1}$)) and of dissolved inorganic carbon (D ,($mmolC.L^{-1}$):

$$\tfrac{1-\alpha}{\alpha} S_2 + \tfrac{1}{\alpha} D \xrightarrow{\mu X} \tfrac{1-\alpha}{\alpha} C + X \tag{5}$$

Where μ is the photosynthesis rate. Here, for sake of simplicity, we assume that photosynthesis and calcification are coupled (see Bernard et al. (2008) for models where these processes are uncoupled). This coupling underlies the fact that the CO_2 released during calcification can be used as a substrate for photosynthesis. The constant α represents the proportion of the total up taken DIC which is allocated to photosynthesis.

The expression of the rate of inorganic carbon acquisition is more tricky; as shown by Droop (1968, 1983), this rate depends on the internal nitrogen quota Q, where $Q = N/X$ is the ratio of particulate phytoplanktonic nitrogen to particulate organic carbon. However, coccolithophorids photosynthesis and calcification are also sensitive to the DIC concentration, and there is a consensus to admit that CO_2 would eventually be the substrate for photosynthesis while

	Value	**Meaning**
α	0.53 –	proportion of DIC for photosynthesis
η_1	0.3 –	fraction of exported POC flux
η_2	0.1 –	fraction of exported POC
μ	. d^{-1}	photosynthesis rate
$\bar{\mu}$	.[1] d^{-1}	max. hypothetical photosynthesis rate
ρ	. $\mu molN.mmolC^{-1}.d^{-1}$	NO_3uptake rate
ρ_m	100.19 $\mu molN.mmolC^{-1}.d^{-1}$	maximum NO_3 uptake rate
I_0	300 $\mu molQ.m^{-2}.s^{-1}$	mean incident light
k_1	0.07 m^{-1}	light extinction rate
k_2	0.05 $m^{-1}.mmolN^{-1}$	light extinction rate
k_{D_p}	.[1] $\mu mol.L^{-1}$†	affinity constant for D_p
k_N	0.038 $\mu mol.L^{-1}$	affinity constant for NO_3
k_{diss}	0.16 d^{-1}	coccolith dissolution rate for $\Omega = 1$
k_d	0.05 d^{-1}	exchange rate through thermocline
K_H	36.7 $mmolCO_2.L^{-1}.\mu$atm	Henry's constant
k_I	50 $\mu molQ.m^{-2}.s^{-1}$	affinity constant for light
k_L	5.87 $dm.d^{-1}$	CO_2 transfer coefficient
k_{sed}	0.05 d^{-1}	sedimentation rate
L	15 m	mixed layer depth
m	0.1 d^{-1}	mortality rate
Q_0	32.29 $\mu molN.mmolC^{-1}$	internal subsistance quota
z	. m	depth

Table 2. Definitions and values of the model parameters. [1]: depends on the model type, see Table 4. †: unitless for Ω.

HCO_3^- would be the substrate for calcification Berry et al. (2002). Therefore the regulation of photosynthesis and calcification could theoretically be triggered by CO_2 or HCO_3^-. In addition, Bernard et al. (2008) examined the possibility that CO_3^{2-} was involved in the regulation of inorganic carbon acquisition, as suggested by recent works Merico et al. (2006). Here, we also consider that availability of calcium can potentially regulate calcification. With this last hypothesis, μ is a function of Ω, the saturation state of calcite ($CaCO_3$):

$$\Omega = \frac{[Ca^{2+}][CO_3^{2-}]}{k_{sp}} \tag{6}$$

where the solubility constant yields $k_{sp} = 5.15\ 10^{-7} mol^2.L^{-2}$.

As a consequence, in the sequel we examine four possible models that only differ by the regulation mechanism of inorganic carbon acquisition:

- CO_2 is the regulating species, and thus $\mu(Q, CO_2)$ is an increasing function of both Q and CO_2 .
- HCO_3^- is the regulating species, and thus $\mu(Q, HCO_3^-)$ is an increasing function of both Q and HCO_3^-.
- CO_3^{2-} is the regulating species, and thus $\mu(Q, CO_3^{2-})$ is an increasing function of both Q and CO_3^{2-}.
- Ω is the regulating factor, and thus $\mu(Q, \Omega)$ is an increasing function of both Q and Ω.

	Value	**Meaning**
$D_{0,380}$	2.07 $mmolC.L^{-1}$	DIC deep concentration (for 380 ppm)
$D_{0,760}$	2.18 $mmolC.L^{-1}$	DIC deep concentration (for 760 ppm)
$S_{1,0}$	5 $\mu molN.L^{-1}$	NO_3deep concentration
$S_{2,0}$	10.4 $mmol\ Ca.L^{-1}$	Ca^{2+} deep concentration

Table 3. Composition of deep seawater.

To keep a general denomination, we denote $\mu_p(Q, D_p)$ the growth rate, where, depending on the model $\mathcal{M}_p$, D_p is chosen among CO_2 , HCO_3^-, CO_3^{2-} and Ω.

The first three models were mathematically studied in Bernard et al. (2008), where the authors analysed qualitative responses to *in vitro* shifts in pCO_2 . Results demonstrated that models ($\mathcal{M}_p$) where D_p was either CO_2 or HCO_3^- supported the results of Iglesias-Rodriguez et al. (2008b), while models where CO_3^{2-} was the regulating factor supported the results obtained by Sciandra et al. (2003).

These biological models are modified here to reproduce more realistic environmental conditions. They now account for light distribution and are used to simulate a more complex *in situ* bloom of *E.huxleyi* in a mixed layer.

2.2 Net carbon fixation rate modelling in a light gradient

As in Bernard et al. (2008), we consider an analytical expression of $\mu_p(Q, D_p)$ based on the Droop model (Droop, 1968, 1983). However, here, the carbon fixation kinetics is completed by two phenomena which cannot be neglected when considering the natural environment: exponential attenuation of light (I) in the seawater and mortality (including respiration and grazing losses). The net growth is now represented by the following function, depending on the the incident irradiance I_0:

$$\mu(Q, D_p, I_0) = \bar{\bar{\mu}}(I_0)(1 - \frac{Q_0}{Q})\frac{D_p}{D_p + k_{D_p}} - m \tag{7}$$

where Q_0 and k_{D_p} are respectively the subsistence quota and the half-saturation constant for the chosen regulating species. The mortality rate m is supposed constant during the short period of time considered for the bloom simulation (typically one month).

The averaged maximal hypothetical growth rate at incident light I_0, denoted $\bar{\bar{\mu}}(I_0)$, is the mean value of the maximum hypothetical growth rate for a light intensity $I(z)$ (denoted $\bar{\mu}(I(z))$) exponentially decreasing along the depth z. We use the following expression, supported *e.g.* by Nimer and Merrett (1993):

$$\bar{\mu}(I) = \bar{\mu}\frac{I}{I + k_I} \tag{8}$$

To compute the maximum hypothetical growth rate averaged on the mixed layer, $\bar{\bar{\mu}}(I_0)$, we take into account the exponential decrease of light with depth. We use the model of Oguz and Merico (2006) assuming that light extinction rate is the sum of a constant rate k_1 (due to the background and suspended material extinction) and, because of the phytoplankton-specific extinction, a rate proportional (with a coefficient k_2) to phytoplanktonic nitrogen N.

$$I(z) = I_0 \exp(-(k_1 + k_2 N)z) \tag{9}$$

We denote $\bar{\bar{\mu}}(I_0)$ the average value of $\bar{\mu}\frac{I(z)}{I(z)+k_I}$ in the mixed layer of depth L. It can then be computed as follows:

$$\bar{\bar{\mu}}(I_0) = \frac{1}{L}\int_0^L \bar{\mu}\frac{I_0 \exp(-(k_1 + k_2 N)z)}{I_0 \exp(-(k_1 + k_2 N)z) + k_I} dz \tag{10}$$

a straightforward computation leads to:

$$\bar{\bar{\mu}}(I_0) = \frac{1}{(k_1 + k_2 N)L} \ln \frac{I_0 + k_I}{I_0 \exp(-(k_1 + k_2 N)L) + k_I} \tag{11}$$

2.3 Inorganic carbon modelling

In order to compute CO_2 , HCO_3^-, $CO_3^{2-}$and Ω from DIC and Ca^{2+} (S_2), classical equations of the seawater carbonate system must be considered (Zeebe and Wolf-Gladrow, 2003; Millero, 2007). We briefly recall these equations.

Dissolved inorganic carbon (denoted D) is defined as the sum of the various inorganic carbon species:

$$D = [HCO_3^-] + [CO_3^{2-}] + [CO_2] \tag{12}$$

The carbonate alkalinity (CA) represents the sum of the electric charges carried in the carbonate system:

$$CA = [HCO_3^-] + 2[CO_3^{2-}] \tag{13}$$

An approximation of the total alkalinity (TA) can be obtained using the expression (see Zeebe and Wolf-Gladrow (2003) for more details) :

$$TA = CA + [B(OH)_4^-] + [OH^-] - [H^+] \tag{14}$$

We denote $\lambda = TA - 2[Ca^{2+}] = TA - 2S_2$. To a first approximation, the ions that most contribute to λ depend on the salinity and remain constant. It is worth noting that total alkalinity is affected by calcification, and must be recomputed at each time point taking into account the calcium:

$$TA = \lambda + 2S_2 \tag{15}$$

To compute inorganic carbon speciation and pH, once dissolved inorganic carbon and calcium are known, a system of equations must be considered on the basis of equations (12) to (14) and of the equilibrium constants of the involved acid/base couples (Zeebe and Wolf-Gladrow, 2003). To solve this system, we used the Matlab code (supplement to Zeebe and Wolf-Gladrow (2003)), which was modified to account for the effects of changes in calcium concentration on the computation of total alkalinity (equation 15).

2.4 Considered simplified physics

In summer, density gradients generated by increasing temperatures lead to water stratification. The surface layer remains mixed over a generally shallow depth. Here we considered a mixed layer depth L of 15m, and to keep the model as simple as possible we assumed, as in Tyrell and Taylor (1996), an homogeneous distribution. We simulated the growth of coccolithophorids in this mixed layer, as represented in Fig. 1. CO_2 concentration in the water equilibrates with that in the atmosphere, following the difference in concentration between the two compartments and according to the diffusion coefficient k_L.

In the water, CO_2 equilibrates with $HCO_3^-$and CO_3^{2-}. The CO_2 pool is also affected by the coccolithophorids activity, being fueled by respiration and consumed through the processes of photosynthesis and calcification (see (5)). The model simulates a nitrate uptake limited by the availability

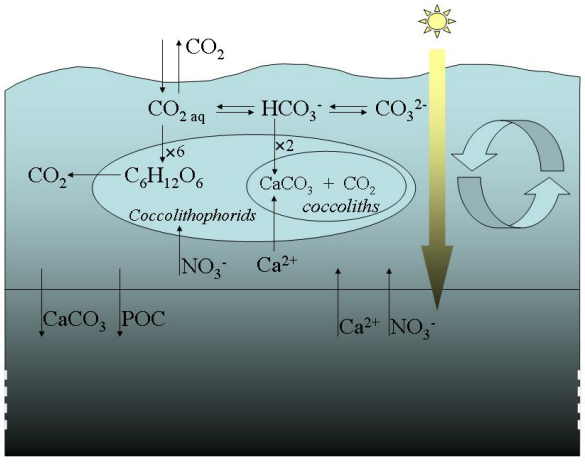

Fig. 1. Schematic diagram of the well mixed upper ocean represented by the model.

of NO_3, as illustrated by equation (3). NO_3, DIC and Ca^{2+} in the mixed water are replenished from the deeper waters (with an exchange rate k_d) whose concentration are respectively $S_{1,0}$, D_0 and $S_{2,0}$. As water acidity affects the coccoliths persistence, we accounted for a possible dissolution of coccoliths whose rate is dependent on pH through the calcite saturation state. We assume that this rate can be written as $\frac{k_{diss}}{\Omega}$, where k_{diss} is the dissolution rate when $\Omega = 1$. Settlement of organic and inorganic particulate carbon is represented through a sinking process below the mixed layer with a sedimentation rate k_{sed}.

2.5 Model equations

The resulting model equations, when considering the presented extension of the models from Bernard et al. (2008) embedded in the simplified considered physics, can now be written as:

$$\dot{S}_1 = k_d(S_{1,0} - S_1) - \rho(S_1)X \tag{16}$$

$$\dot{Q} = \rho(S_1) - \mu(Q, D_p, I_0)Q \tag{17}$$

$$\dot{X} = -k_d X + \mu(Q, D_p)X - mX - k_{sed}X \tag{18}$$

$$\dot{C} = -k_d C + \frac{1-\alpha}{\alpha}\mu(Q, D_p, I_0)X - k_{sed}C - \frac{k_{diss}}{\Omega}C \tag{19}$$

$$\dot{D} = k_d(D_0 - D) - \frac{1}{\alpha}\mu(Q, D_p, I_0)X + RX \tag{20}$$

$$-k_L(CO_2 - k_H pCO_2) + \frac{k_{diss}}{\Omega}C \tag{21}$$

$$\dot{S}_2 = k_d(S_{2,0} - S_2) - \frac{1-\alpha}{\alpha}\mu(Q, D_p, I_0)X \tag{22}$$

D_p is the regulating factor (among CO_2 , HCO_3^-, $CO_3^{2-}$and Ω) assumed to control both photosynthesis and calcification.

The initial conditions have been chosen assuming that coccolithophorids bloom right after a large diatom bloom which reduced the nitrate and inorganic carbon concentrations in the mixed layer (Riebesell et al., 1993). According to real pCO_2 data observed during *in situ* bloom experiments (Keeling et al., 1996; Benthien et al., 2007), we consider that 0.2 mmol.L^{-1} of total inorganic carbon was consumed by the previous bloom. The reference (i.e. before the diatom bloom) dissolved inorganic carbon concentration was computed assuming an equilibrium with the atmosphere (see Table 3).

2.6 Export computation

The exported carbon flux is computed at two different times. First, during the bloom, equations (16) to (22) are numerically integrated using the Matlab solver *ode15s* (Shampine and Reichelt, 1997). The flux follows the material export to the deep layer, through the processes of sedimentation and exchange through the thermocline. The end of the bloom occurs after 20 days; in this second phase, we assume that an unmodelled process, *i.e.* a high cell lysis or a strong predation event, makes *E. huxleyi* disappear within ten days, concomitantly to a high transparent exopolymer particles (TEP) production (Engel et al., 2004; Harlay et al., 2009). The dynamics of this process is not represented, but from a macroscopic point of view we assume that it leads to the transformation of the PIC and POC reached at the end of the bloom into settling particles. We estimated the fraction of exported carbon from studies on the link between primary production and organic export (De La Rocha and Passow, 2007; Boyd and Trull, 2007). Last, representing the export of coccoliths is far from trivial, as this complex phenomenon is neither clearly understood nor quantitatively described yet. The main export mechanism would be related to particles aggregation, mainly fecal pellets, which is also enhanced with TEP abundance (De La Rocha and Passow, 2007; Boyd and Trull, 2007; Harlay et al., 2009) and can be enhanced in conditions of nitrate limitation (Corzo et al., 2000; Engel et al., 2004). Let us keep in mind that our goal is not to provide an exhaustive description of this mechanism, but to catch a realistic range of magnitude with our simplified model.

2.6.1 Export carbon computation during the bloom

During *E.huxleyi* growth, the carbon flux is proportional to the material exported to the deep layer. The average exported POC during the 20 days of the bloom can thus be computed as follows:

$$F^1_{\mathrm{POC}} = \frac{\eta_1 L}{20}\int_0^{20}(k_d + k_{sed})X(t)dt \quad (23)$$

where η_1 is the fraction of POC non locally degraded (De La Rocha and Passow, 2007).

To compute the exported PIC, we refer to the estimate proposed by Ridgwell et al. (2007), assuming that it is related to the POC flux with a carrying capacity of organic aggregates for minerals (Passow and De la Rocha, 2006), and that a fraction, depending on Ω, may be dissolved. The mean flux during the 20 days of the bloom then reads (with parameters as in Ridgwell et al. (2007)):

$$F^1_{\mathrm{PIC}} = \frac{0.044\eta_1 L}{20}\int_0^{20}(\Omega-1)^{0.32}(k_d + k_{sed})X(t)dt \quad (24)$$

2.6.2 Export carbon computation after the bloom

As the coccolithophorid bloom declines, a high quantity of TEP is produced (Engel et al., 2004; Harlay et al., 2009), which triggers the efficiency of particle coagulation and formation of macroscopic aggregates (Logan et al., 1995; De La Rocha and Passow, 2007; Kahl et al., 2008). We assume that TEP is related to the remaining POC at the final time of the simulation (*i.e.* when the bloom starts to decline).

The average daily POC flux during the ten days following the bloom is assumed to be a fraction η_2 of the remaining primary production at the end of the bloom:

$$F^2_{\mathrm{POC}} = \frac{\eta_2 L}{10}POC(t=20) \quad (25)$$

The same expression as equation (24) based on the formulation of Ridgwell et al. (2007) is used to compute the exported PIC:

$$F^2_{\mathrm{PIC}} = \frac{0.044\eta_2 L}{10}(\Omega-1)^{0.32}POC(t=20) \quad (26)$$

3 Model simulation

3.1 Model calibration

Depending on the choice of the regulating inorganic carbon variable D_p, four different models result from the different hypotheses as for the mechanisms driving both photosynthesis and calcification. Even if the objective is to sketch a generic bloom of *E.huxleyi*, the models were carefully calibrated using realistic parameter values, as detailed in the following.

Temperature and salinity are 15°C and 35g/kg^{-1}, respectively. The residence time in the mixed layer is assumed to be 20 days (Schmidt et al., 2002), while the sedimentation rate k_{sed} was computed using an average coccolith sedimentation rate of $0.75m/day$ (Gregg and Casey, 2007). The dissolution constant k_{diss} was computed so that the calcite dissolution rate in standard pCO_2 conditions is $0.75d^{-1}$ (Oguz and Merico, 2006). The DIC deep concentration is assumed to be related to atmospheric pCO_2 , and depending on the considered pCO_2 scenario, three values will be considered,

denoted $D_{0,380}$, $D_{0,760}$ and $D_{0,1140}$. The fraction of POC exported to the deep layer during the bloom ($\eta_1 = 0.3$) and the fraction of the remaining POC exported during the declining phase ($\eta_2 = 0.1$) have been calibrated using ranges provided by Honjo et al. (2008).

The nitrogen uptake rate is derived from Bernard et al. (2008), together with the values of the half saturation constants k_{D_p} (according to Rost and Riebesell (2004), see Table 4). The light extinction coefficients are computed from Oguz and Merico (2006). The values for the half saturation constants k_{D_p} are taken from Bernard et al. (2008).

The maximum exponential growth rate under non limiting conditions can be computed from the maximum hypothetical growth rate (Bernard and Gouzé, 1995):

$$\mu_{max}(I, D_p) = \bar{\mu}(I) \frac{D_p \rho_m}{Q_0 \bar{\mu}(I) D_p + \rho_m (D_p + k_{D_p})} \quad (27)$$

and thus we can get $\bar{\mu}(I)$ from $\mu_{max}(I)$:

$$\bar{\mu}(I) = \frac{\rho_m \mu_{max}(I, D_p)}{\rho_m - Q_0 \mu_{max}(I, D_p)} (1 + \frac{k_{D_p}}{D_p}) \quad (28)$$

The values for $\mu_{max}(I, D_p)$ are taken from Gregg and Casey (2007), using our values of temperature and half saturation constant for light intensity. We assume that this growth rate is obtained under nowaydays pCO_2 (380ppm) associated to standard CO_2 , HCO_3^-, $CO_3^{2-}$and Ω computed using standard seawater values (Zeebe and Wolf-Gladrow, 2003). This provides the values of $\bar{\mu}(I)$ for each of the four proposed models.

Finally, the set of nominal parameter values are presented in Tables 2 and 4. The considered seawater composition is presented in Table 3.

At this stage, we can remark that models regulated by $CO_3^{2-}$and Ω present similar behaviours (data not shown). Indeed the simulations show very close predictions that always differ by less than 1%. This fact is consequent to the stability of Ca^{2+} concentration in surface seawater, which makes Ω proportional to CO_3^{2-}along the simulation. Note that this property is not straightforward for *in vitro* experiments (especially in batch conditions) where the high biomass level may affect the Ca^{2+} stock, and thus more drastically influence Ω.

In the sequel we will therefore only consider the model in which the calcite saturation state is the regulating factor.

3.2 Monte Carlo simulations

In order to assess the effect of the parameter uncertainty and their possible variations during the bloom, Monte Carlo simulations are performed from randomly parameter values. The probability distribution of the parameters is supposed to be Gaussian, centered on the nominal value (See Tables 2 and 4), and with a standard deviation of 10% of the nominal value (*i.e.* 95% of the parameter values are in the interval $\pm 20\%$ of their nominal value). 1000 random parameter sets are chosen, and for each set a simulation is run. The average prediction together with its standard deviation is then computed.

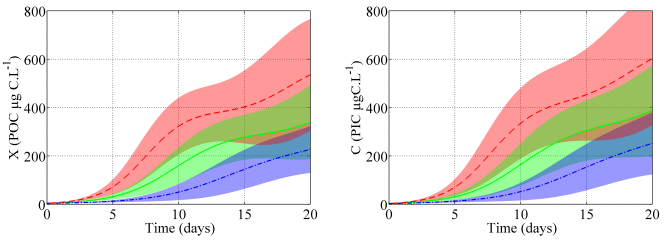

Fig. 2. Simulated POC and PIC at pCO_2 =380ppm with the three models differing by the considered regulating variable D_p (CO_2 : _ . _, HCO_3^-:— and Ω: - -). Colored area represent the corresponding standard deviation.

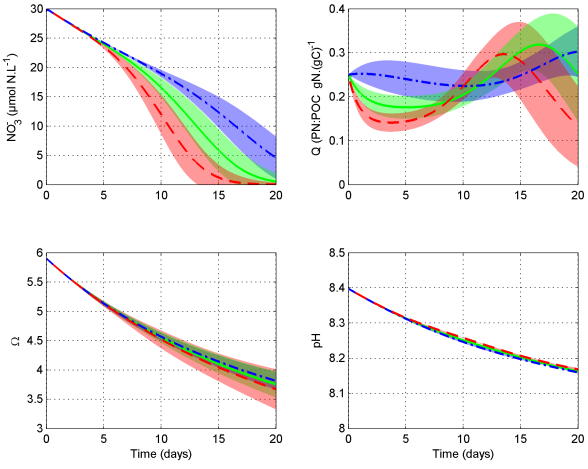

Fig. 3. Simulated nitrate concentration, internal nitrogen quota, calcite saturation state and pH at pCO_2 =380ppm, depending on the considered regulating variable D_p (CO_2 : _ . _, HCO_3^-:— and Ω: - -). Colored area represent the corresponding standard deviation.

3.3 Simulation at nowadays pCO$_2$

We used each of the three models to simulate a large bloom of *Emiliania huxleyi*. Phytoplankton cells are assumed to grow in a homogeneous layer, where aqueous CO_2 equilibrates with the atmosphere. It takes several weeks to supply inorganic carbon from both atmosphere and the deeper ocean to the cells in the whole mixed layer, and to reconstitute the

Parameters	CO_3^{2-}	HCO_3^-	CO_2	Ω	Units
k_{D_p}	0.16	1.65	0.015	3.23†	$\mu molC.L^{-1}$
$\bar{\mu}$	1.34	0.96	1.7	1.64	d^{-1}

Table 4. Kinetics parameters depending on the chosen model. († unitless for k_Ω)

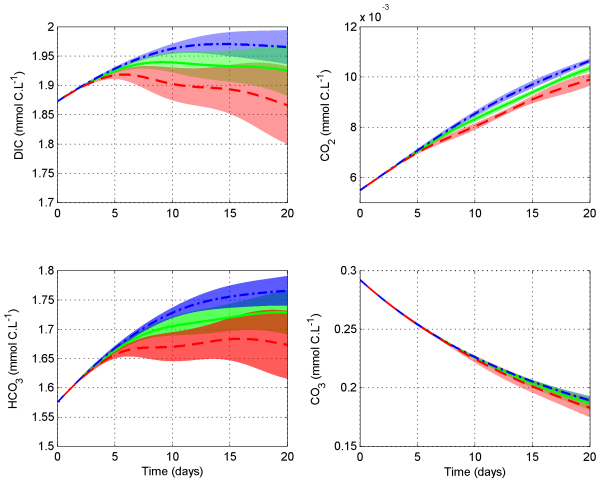

Fig. 4. Simulated inorganic carbon with the three models at pCO_2 =380ppm differing by the considered regulating variable D_p (CO_2 : _ . _, HCO_3^-:— and Ω: - -). Colored area represent the corresponding standard deviation.

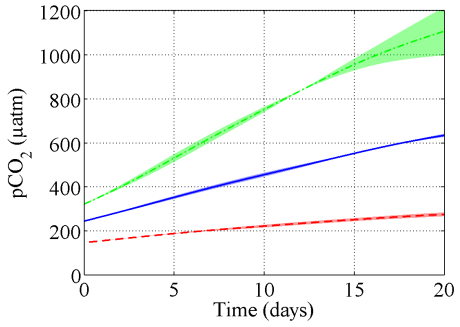

Fig. 5. Seawater pCO_2 averaged along the three considered models, for the three considered atmospheric pCO_2 (380 ppm: - - - , 760 ppm: :— and 1140 ppm: _ . _). Colored area represent the corresponding standard deviation.

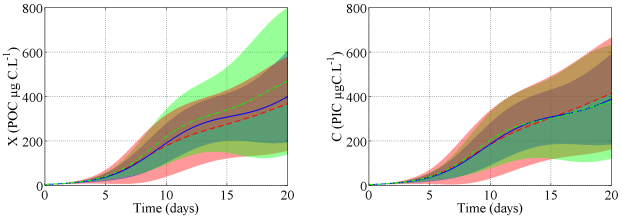

Fig. 6. PIC and POC averaged along the three considered models, for the three considered atmospheric pCO_2 (380 ppm: - - - , 760 ppm: :— and 1140 ppm: _ . _). Colored area represent the corresponding standard deviation.

stock of inorganic carbon depleted by the previous bloom (Figures 3 and 4). The inorganic carbon stock reconstitution is slowed down by the consumption of inorganic carbon by the *E. huxleyi* bloom. As a consequence, during the simulation, $CO_3^{2-}$and Ω show higher values, while CO_2 and $HCO_3^-$are lower compared to their respective steady state value. This fact can explain the significantly different behaviours observed between the 3 models (Figure 4). Indeed, it turns out that because of the high consumption of CO_2 by the blooming biomass, the progressive depletion of inorganic carbon results in a stronger down regulation of photosynthesis and calcification in models controlled by CO_2 or HCO_3^-. On the contrary, the models regulated by CO_3^{2-}or Ω are enhanced by the depletion in inorganic carbon. It results that the predicted, fixed carbon during the bloom formation is twofold in the $CO_3^{2-}$and Ω models compared to the CO_2 model (Figure 2).

3.4 Simulation with doubled pCO$_2$

Based on the accumulation rate of CO_2 observed in the atmosphere from the beginning of the industrial era, current models roughly predict a pCO_2 doubling. Since the atmosphere tends to be in equilibrium with the superficial oceanic layers, changes in atmospheric CO_2 directly affect the CO_2 seawater concentration, and consequently the carbonate system speciation.

Under such conditions of elevated pCO_2 , the initial condition of depleted inorganic carbon concentration in the water column, due to the development of the previous bloom, is transiently observed and still appears more favorable to the $CO_3^{2-}$and Ω models (data not shown). However this tendency does not last, since inorganic carbon rapidly increases as CO_2 in the water equilibrates with the elevated values of both atmosphere and deep layer (see Figure 5). After one week, ambient conditions are back to high CO_2 concentrations and then prove to be much more favorable to the CO_2 and HCO_3^-models which induce stimulated inorganic carbon uptake and rapidly recover. Yet, important differences appear in the final PIC and POC concentrations, with higher predicted values in the CO_2 model (see Table 5).

4 Discussion

4.1 Modelling choices

The objective of this work was to explore the effect of the dynamical nature of the considered processes on the carbon fluxes predictions. A a consequence, this work does not assume a constant pCO_2 in the seawater, contrary to most of the studies dealing with the impact of pCO_2 increase. Indeed, our models represent the pCO_2 variation due the coc-

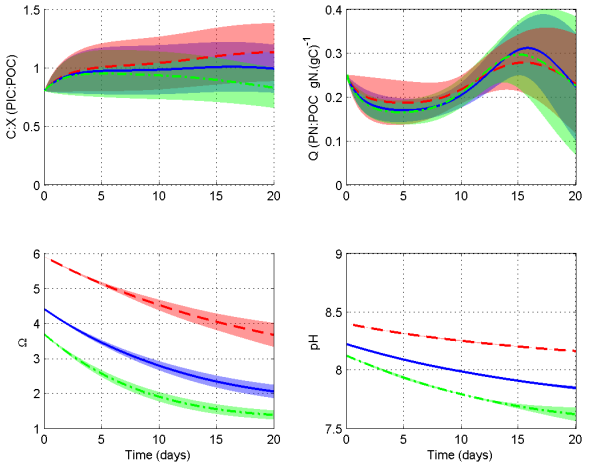

Fig. 7. PIC:POC, PN:POC, Ω and pH averaged along the three considered models, for the three considered atmospheric pCO_2 (380 ppm: - - -, 760 ppm: :— and 1140 ppm: _ . _). Colored area represent the corresponding standard deviation.

pCO_2 (ppm)	$\mathcal{M}$ CO_2	$\mathcal{M}$ HCO_3^-	$\mathcal{M}$ Ω	CV/$\mathcal{M}$ (%)
		PIC (t=20) μg/l		
380	245.5 (45.4)	401.0 (48.3)	605.6 (44.9)	(60.1)
760	501.6 (48.4)	387.2 (50.9)	296.4 (50.3)	(54.9)
1140	634.7 (34.3)	353.9 (45.4)	150.3 (47.6)	(67.4)
CV/pCO_2	(*62.9*)	(*55.9*)	(*85.5*)	
		POC (t=20) μg/l		
380	222.3 (37.6)	349.4 (46.2)	538.2 (43.3)	(58.0)
760	518.4 (44.7)	389.6 (47.0)	298.3 (50.9)	(52.7)
1140	817.7 (33.5)	430.2 (44.2)	176.2 (44.7)	(69.4)
CV/pCO_2	(*63.3*)	(*47.9*)	(*67.2*)	
		$F_{PIC} + F_{POC}$ (t=20) $mg/m^2/d$		
380	11.8 (39.2)	18.6 (48.0)	28.6 (44.3)	(58.9)
760	27.1 (45.8)	20.3 (47.5)	15.7 (51.5)	(53.4)
1140	41.9 (35.0)	22.2 (45.3)	9.1 (46.2)	(70.0)
CV/pCO_2	(*62.2*)	(*47.4*)	(*67.9*)	

Table 5. Final values of PIC and POC at t=20 days, and average daily exported carbon during the bloom, in $mgC.m^{-2}.d^{-1}$ with respect to the considered model and pCO_2 . In brackets: CV (Coefficient of variation), expressed in %.

colithophorid bloom which consumes both inorganic carbon and alkalinity. We have thus chosen to detail the phenomena within the time scale of the bloom, and especially those which are likely to vary with respect to a pCO_2 change. As a consequence, we have assumed that mortality (due to predation (Garcia et al., 2008), viruses (Jacquet et al., 2002), ...) was constant during 20 days, and that *Emiliania huxleyi* was dominating the phytoplankton community during this period. The important point is that these phenomena of slower dynamics are not directly influenced by the pCO_2 and can therefore reasonably be considered to be of similar intensities for various pCO_2 scenarii. Focusing on the pCO_2 dependent biological and chemical processes, we can thus compare different pCO_2 situations under the hypotheses that they are comparable since the non represented phenomena have a similar effect. In the same spirit, we have not represented the strong mechanisms (predation or viruses) that transform, within 10 days, the living cells of *E.huxleyi* into settling organic and inorganic matter. We assume therefore that the predation process will be rather unaffected by the pCO_2 , so that that its global efficiency to transform biomass into exported material is only impacted by the saturation state of calcite Ω through inorganic carbon export expressions (24) and (26) (Ridgwell et al., 2007). It is however likely that this assumption introduces a bias since the link between POC concentration and TEP production is probably pCO_2 dependent (Engel, 2002; Engel et al., 2004; Riebesell et al., 2007), and thus parameters η_2 should be an increasing function of TEP. However, in the models where photosynthesis and calcification are stimulated by an increase in pCO_2 , even if this effect is not represented, a higher POC is produced leading to higher carbon export.

4.2 Hypothesis of a regulation based on calcite saturation state

The new biological model that we introduced, in which the calcite saturation state drives calcification, turns out to be an alternative explanation to the CO_3^{2-}model. This model assumes that the calcite saturation state, even when higher than 1 (meaning that dissolution rate is low), strongly influences the calcification rate. The simulations illustrate a property that could have been shown analytically, using similar principles than in Bernard et al. (2008): the Ω follows the CO_3^{2-}model. This model can thus explain the experimental results obtained by Sciandra et al. (2003). In the hypothesis of uncoupled calcification and photosynthesis, if Ω is used to control the calcification rate while the photosynthesis rate is driven by CO_2 , then the experimental results of Riebesell et al. (2000) can be reproduced. This results holds for *in situ* considerations since calcium in the mixed layer is only marginally affected by the bloom. However, this conclusion may not hold for the high biomasses reached in *in vitro* experiments.

It is worth remarking that the models only focus on the factor impacting growth and calcification. They do not assume any hypothesis on the nature of the inorganic carbon species which is consumed. Indeed, the models globally represent the uptake in the inorganic carbon D compartment. When a mole of inorganic carbon is consumed (whatever the species), the chemical equilibria are displaced. As a consequence, in this approach, only the regulating factor nature is uncertain.

4.3 Outcome of two opposite effects

The simulations turn out to show that the production and export predictions are the consequence of two antagonist effects.

The first effect is related to the fact that, at higher pCO_2, the HCO_3^- and CO_2 models predict an enhanced uptake of dissolved inorganic carbon, compared to the model regulated through Ω. From a quantitative point of view, the magnitude of this phenomenon relies on the way models are calibrated. They all predict the same photosynthesis and calcification rates for 380 ppm and standard alkalinity. This reference situation, for which many data are available, was used to calibrate most of the parameters. The second effect turns out to be the opposite of the direct effect: for pCO_2 lower than 380, *i.e.* right after the diatom bloom, the photosynthesis and calcification rates of the HCO_3^- and CO_2 models is lower because of the inorganic carbon depletion in the water column. On the contrary, for the model enhanced by Ω, the first ten days of the bloom are in highly favorable conditions and thus both POC and PIC production are enhanced. Finally, whatever the considered model, the first ten days of the bloom and the last ten days lead to opposite inorganic carbon uptake conditions. This compensation phenomenon is probably the key reason why, in the end, the prediction difference between the models is strongly reduced. Despite this effect due to depletion of the inorganic carbon when the bloom takes place, as indicated by the figures in Table 5, the CO_2 and Ω models predict a two-fold difference in the final PIC and POC concentrations under a doubled pCO_2 .

4.4 Can we predict the effect of a pCO_2 increase ?

Here, simulations suggest that a change in pCO_2 will impact coccolithophorid bloom formation. Yet, depending on the model, this variation is an increase (see the doubling in PIC in the CO_2 model) or a decrease (see the 50 % PIC drop in the Ω model). Hence, simulations also point out two-fold differences in these predicted concentrations, depending on the considered regulating factor. That is, the variability in the predicted values, observed between the models, equals or even exceeds that due to the rise in pCO_2 . This statement is reinforced when considering a tripling of pCO_2 (see Table 5). This point is absolutely critical as it demonstrates the strong dependence of the model outcome on the initial hypotheses made as for the regulation of photosynthesis and calcification.

Figures 6 and 7 present the averaged simulations of the three different models (each curve thus corresponds to 3000 simulations) as a response to pCO_2 . It is remarkable that the average predictions seem to be rather unaffected by the pCO_2 value: without a firm hypothesis on the regulation mechanisms, no effect of a pCO_2 shift can be estimated. When considering Figure 7, the only prediction that seems to hold for the whole set of models is the decrease of the PIC:POC ratio when increasing the pCO_2 , which is a direct consequence of increased coccolith dissolution.

The phenomena, revealed by our short time scale approach, are likely to appear when dealing with models designed to simulate longer terms dynamics, including more accurate interactions with the whole ecosystem. The tight dependence of the stock and flux predictions on the underlying regulation mechanisms and the paradoxical effect due to the inorganic carbon depletion after the diatom bloom may both strongly affect any modelling prediction. So far, to our knowledge, none of the complex models dealing with coccolithophorids (Tyrell and Taylor, 1996; Merico et al.; Oguz and Merico, 2006; Gregg and Casey, 2007) accurately represent inorganic carbon dynamics and its impact on the biological kinetics. As stated by Riebesell (2004), it seems impossible at this point to provide any reliable forecast of large-scale and long-term biological responses to global environmental change. Our study should therefore be considered as a methodological approach on a bench model to highlight a phenomenon that will take place in more detailed models (including food web interactions). As more experimental works are needed to unravel the carbon acquisition modes and their regulation in coccolithophorids, prediction statements should be made with caution and discussed in regard to the plausible hypotheses.

Last, another hypothesis was recently brought forward by several authors: the calcification mechanisms also seems to be highly strain dependent (Fabry, 2008; Langer et al., 2009). As an assemblage of various strains (with different carbon acquisition regulation mechanisms), a natural population would then show a range of different responses to increases in pCO_2 . To provide an accurate, simulated response to pCO_2 change, a model should then represent each subpopulation, with various responses to carbonate chemistry, so that the resulting overall response reveals to be a combination of the subpopulation behaviours. Our Monte Carlo simulation approach can also be interpreted as a way to reproduce this natural variability. It then shows that this variability also induces large uncertainties in the flux predictions. We considered parameter variability with a 10% variation coefficient, and it resulted in more than 100% variability in the predictions of particulate stocks and fluxes.

5 Conclusions

The originality of this work is to consider the dynamics of both carbonate system and inorganic carbon uptake and their coupling. As a consequence, our models point out the transient periods during which the inorganic carbon is much lower than its value at equilibrium with atmosphere. During these transient phases, the scenarii in which CO_3^{2-} or Ω regulate calcification and photosynthesis may be strongly advantaged, leading thus to an unexpected effect which highly attenuates the direct effect of pCO_2 increase.

This study stresses how correct identification of the chemical species that drive calcification and photosynthesis processes is critical for accurate predictions of coccolithophorid blooms and for the estimation of the consequent amount of carbon withdrawn from the atmosphere and trapped into the deep ocean. Model results reveal a striking difference in the predicted biomass increase when the saturation state Ω (or equivalently CO_3^{2-}) is the regulating factor compared to the CO_2 model.

A detailed validated model including interactions with a trophic network may allow predictions at larger time scale, especially for carbon export, but it may also be affected by the same uncertainties that our bench model, thus resulting in highly uncertain predictions of carbon fluxes in the situations of large blooms of coccolithophorids.

Results thus strongly call for further experimental approaches to more accurately identify the chemical species that primarily regulate photosynthesis and calcification.

Acknowledgements. The authors benefited from the support of the European FP7 Integrated Project EPOCA (European Project on OCean Acidification), and of the Remecca project within the GIS Oceanomed (Total fundation).

References

Benthien, A., Zondervan, I., Engel, A., Hefter, J., Terbüggen, A., and Riebesell, U.: Carbon isotopic fractionation during a mesocosm bloom experiment dominated by *Emiliania huxleyi*: Effects of CO_2 concentration and primary production, Geochimica et Cosmochimica Acta, 71, 1528–1541, 2007.

Bernard, O. and Gouzé, J. L.: Transient Behavior of Biological Loop Models, with Application to the Droop Model, Mathematical Biosciences, 127, 19–43, 1995.

Bernard, O., A.Sciandra, and Madani, S.: Multimodel analysis of the response of the coccolithophore *Emiliania huxleyi* to an elevation of pCO_2 under nitrate limitation , Ecol. Model., 211, 324–338, 2008.

Berry, L., Taylor, A. R., Lucken, U., Ryan, K. P., and Brownlee, C.: Calcification and inorganic carbon acquisition in coccolithophores., Funct Plant Biol, 29, 1–11, 2002.

Boyd, P. and Trull, T.: Understanding the export of biogenic particles in oceanic waters: Is there consensus?, Progress In Oceanography, 72, 276 – 312, 2007.

Buitenhuis, E. T., de Baar, H. J. W., and Veldhuis, M. J. V.: Photosynthesis and calcification by *Emiliania huxleyi* (Prymnesiophyceae) as a function of inorganic carbon species., J Phycol, 35, 949–959, 1999.

Burmaster, D.: The unsteady continuous culture of phosphate-limited *Monochrisis lutheri Droop* : Experimental and theoretical analysis., Journal of Experimental Marine Biology and Ecology, 39 (2), 167–186, 1979.

Corzo, A., Morillo, J., and Rodriguez, S.: Production of transparent exopolymer particles (TEP) in cultures of *Chaetoceros calcitrans* under nitrogen limitation, Aquatic Microbial Ecology, 23, 63–72, 2000.

De La Rocha, C. and Passow, U.: Factors influencing the sinking of POC and the efficiency of the biological carbon pump, Deep Sea Research Part II: Topical Studies in Oceanography, 54, 639 – 658, 2007.

Droop, M. R.: Vitamin B12 and marine ecology. IV. The kinetics of uptake growth and inhibition in *Monochrysis lutheri*, J. Mar. Biol. Assoc., 48, 689–733, 1968.

Droop, M. R.: 25 Years of Algal Growth Kinetics, A Personal View, Botanica marina, 16, 99–112, 1983.

Dugdale, R. C.: Nutrient limitation in the sea: dynamics, identification and significance, Limnol. Oceanogr., 12, 685–695, 1967.

Engel, A.: Direct relationship between CO2 uptake and transparent exopolymer particles production in natural phytoplankton, JOURNAL OF PLANKTON RESEARCH, 24, 49–53, 2002.

Engel, A., Delille, B., Jacquet, S., Riebesell, U., Rochelle-Newall, E., Terbruggen, A., and Zondervan, I.: Transparent exopolymer particles and dissolved organic carbon production by *Emiliania huxleyi* exposed to different CO2 concentrations: a mesocosm experiment, Aquatic Microbial Ecology, 34, 93–104, 2004.

Fabry, V. J.: Ocean science - Marine calcifiers in a high-CO2 ocean, Science, 320, 1020–1022, 2008.

Falkowski, P. G.: Evolution of the nitrogen cycle and its influence on the biological sequestration of CO2 in the ocean, Nature, 327, 242–244, 1997.

Frankignoulle, M., Canon, C., and Gattuso, J. P.: Marine calcification as a source of carbon dioxide: positive feedback of increasing atmospheric CO2, Limnol Oceanogr, 39, 458–462, 1994.

Garcia, V. M. T., Garcia, C. A. E., Mata, M. M., Pollery, R. C., Piola, A. R., Signorini, S. R., McClain, C. R., and Iglesias-Rodriguez, M. D.: Environmental factors controlling the phytoplankton blooms at the Patagonia shelf-break in spring, Deep-Sea Research Part I, 55, 1150–1166, 2008.

Gregg, W. W. and Casey, N. W.: Modeling coccolithophores in the global oceans, Deep-Sea Research Part II , 54, 447–477, 2007.

Harlay, J., Bodt, C. D., Engel, A., Jansen, S., d'Hoop, Q., Piontek, J., Oostende, N. V., Groom, S., Sabbe, K., and Chou, L.: Abundance and size distribution of transparent exopolymer particles (TEP) in a coccolithophorid bloom in the northern Bay of Biscay, Deep Sea Research Part I: Oceanographic Research Papers, In Press, Corrected Proof, –, 2009.

Honjo, S., Manganini, S. J., Krishfield, R. A., and Francois, R.: Particulate organic carbon fluxes to the ocean interior and factors controlling the biological pump: A synthesis of global sediment trap programs since 1983, Progress In Oceanography, 76, 217 – 285, 2008.

Houghton, J. T., Jenkins, G. J., and Ephtraims, J. J.: Climate Change 1995, The Science of Climate Change, Cambridge University Press, 1996.

Iglesias-Rodriguez, M. D., Buitenhuis, E. T., Raven, J. A., Schofield, O., Poulton, A. J., Gibbs, S., Halloran, P. R., and de Baar, H. J. W.: Response to Comment on "Phytoplankton Calcification in a High-CO2 World", Science, 322, 2008a.

Iglesias-Rodriguez, M. D., Halloran, P. R., Rickaby, R. E. M., Hall, I. R., Colmenero-Hidalgo, E., Gittins, J. R., Green, D. R. H., Tyrrell, T., Gibbs, S. J., von Dassow, P., Rehm, E., Armbrust, E. V., and Boessenkool, K. P.: Phytoplankton calcification in a high-CO2 world, Science, 320, 336–340, 2008b.

Jacquet, S., Heldal, M., Iglesias-Rodriguez, D., Larsen, A., Wilson, W., and Bratbak, G.: Flow cytometric analysis of an Emiliana huxleyi bloom terminated by viral infection, Aquatic Microbial Ecology, 27, 111–124, 2002.

Kahl, L., Vardi, A., and Schofield, O.: Effects of phytoplankton physiology on export flux, Marine Ecology Progress Series, 354, 3–19, 2008.

Keeling, R. F., Piper, S. C., and Heimann, M.: Global and hemispheric CO2 sinks deduced from changes in atmospheric O2 concentration, Nature, 381, 308–341, 1996.

Klepper, O., de Haan, B. J., and van Huet, H.: Biochemical feedbacks in the oceanic carbon cycle, Ecol. Modelling, 75, 459–469, 1994.

Langer, G., Nehrke, G., Probert, I., Ly, J., and Ziveri, P.: Strain-specific responses of *Emiliania huxleyi* to changing seawater carbonate chemistry, Biogeosciences Discussions, 6, 4361–4383, http://www.biogeosciences-discuss.net/6/4361/2009/, 2009.

Leonardos, N. and Geider, R. J.: Elemental and biochemical composition of Rhodomonas reticulata (Cryptophyta) in relation to light and nitrate-to-phosphate supply ratios, J. Phycol., 41, 567–576, 2005.

Leonardos, N., Read, B., Thake, B., and Young, J. R.: No mechanistic dependence of photosynthesis on calcification in the coccolithophorid *Emiliania huxleyi* (haptophyta) , J. Phycol., 45, 1046–1051, 2009.

Logan, B. E., Passow, U., Alldredge, A. L., Grossartt, H.-P., and Simont, M.: Rapid formation and sedimentation of large aggregates is predictable from coagulation rates (half-lives) of transparent exopolymer particles (TEP), Deep Sea Research Part II: Topical Studies in Oceanography, 42, 203 – 214, 1995.

Merico, A., Tyrrell, T., Lessard, E., Oguz, T., Stabeno, P., Zeeman, S., and Whitledge, T.: Modelling phytoplankton succession on the Bering Sea shelf: role of climate influences and trophic interactions in generating *Emiliania huxleyi* blooms 1997-2000, Deep-Sea Res. Part I.

Merico, A., Tyrrell, T., and Cokacar, T.: Is there any relationship between phytoplankton seasonal dynamics and the carbonate system?, J. Mar. Syst. , 59, 120–142, 2006.

Millero, F.: The Marine Inorganic Carbon Cycle, Chem.Rev, 107, 308–341, 2007.

Nimer, N. and Merrett, M.: Calcification rate in *Emiliania huxleyi* Lohmann in response to light, nitrate and availability of inorganic carbon, New Phytol., 123, 673–677, 1993.

Nimer, N. A. and Merrett, M. J.: The development of a CO2-concentrating mechanism in *Emiliania huxleyi*., New Phytol, 133, 387–389, 1996.

Oguz, T. and Merico, A.: Factors controlling the summer *Emiliania huxleyi* bloom in the Black Sea: A modeling study, Journal Of Marine Systems, 59, 173–188, 2006.

Orr, J., Fabry, V., Aumont, O., Bopp, L., Doney, S., Feely, R., Gnanadesikan, A., Gruber, N., Ishida, A., Joos, F., Key, R., Lindsay, K., Maier-Reimer, E., Matear, R., Monfray, P., Mouchet, A., Najjar, R., Plattner, G., Rodgers, K., Sabine, C., Sarmiento, J., Schlitzer, R., Slater, R., Totterdell, I., Weirig, M., Yamanaka, Y., and Yool, A.: Anthropogenic ocean acidification over the twenty-first century and its impact on calcifying organisms, Nature, 437, 681–686, 2005.

Paasche, E.: A tracer study of the inorganic carbon uptake during coccolith formation and photosynthesis in the coccolithophorid *Coccolithus huxleyi*., Physiol Plant, 3, 1–82, 1968.

Paasche, E.: A review of the coccolithophorid *Emiliania huxleyi* (Prymnesiophyceae), with particular reference to growth, coccolith formation, and calcification-photosynthesis interaction., Phycologia, 40, 503–529, 2002.

Passow, U. and De la Rocha, C.: Accumulation of mineral ballast on organic aggregates, Global Biogeochemical Cycles, 20, 2006.

Ridgwell, A., Zondervan, I., Hargreaves, J. C., Bijma, J., and Lenton, T. M.: Assessing the potential long-term increase of oceanic fossil fuel CO2 uptake due to CO2-calcification feedback, Biogeosciences, 4, 481–492, 2007.

Riebesell, U.: Effects of CO_2 Enrichment on Marine Phytoplankton, J. Oceanography, 60, 719–729, 2004.

Riebesell, U., Zondervan, I., Rost, B., Tortell, P., Zeebe, R. E., and Morel, F. M. M.: Reduced calcification of marine plankton in response to increased atmospheric CO2., Nature, 407, 364–367, 2000.

Riebesell, U., Wolf-Gladrow, A., and Smetacek, V.: Carbon dioxide limitation of marine phytoplankton growth rates , Science, 361, 249–251, 1993.

Riebesell, U., Bellerby, R. G. J., Engel, A., Fabry, V. J., Hutchins, D. A., Reusch, T. B. H., Schulz, K. G., and Morel, F. M. M.: Comment on "Phytoplankton Calcification in a High-CO2 World", Science, 322, 2008.

Riebesell, U., Schulz, K., Bellerby, R., Botros, M., Fritsche, P., Meyerhofer, M., Neill, C., Nondal, G., Oschlies, A., Wohlers, J., and Zollner, E.: Enhanced biological carbon consumption in a high CO2 ocean, Nature, 450, 545–548 , 2007.

Rost, B. and Riebesell, U.: Coccolithophores and the biological pump: responses to environmental changes., pp. 99–127, Springer, Berlin, 2004.

Rost, B., Riebesell, U., Burkhardt, S., and Sultemeyer, D.: Carbon acquisition of bloom-forming marine phytoplankton., Limnol Oceanogr, 48, 44–67, 2003.

Rost, B., Riebesell, U., and Sultemeyer, D.: Carbon acquisition of marine phytoplankton: Effect of photoperiod length, Limnology and Oceanography, 51, 12–20, 2006.

Schmidt, S., Chou, L., and Hall, I.: Particle residence times in surface waters over the north-western Iberian Margin: comparison of pre-upwelling and winter periods, Journal Of Marine Systems, 32, 3–11, 2002.

Sciandra, A., Harlay, J., Lefévre, D., Lemée, R., Rimmelin, P., Denis, M., and Gattuso, J.-P.: Response of coccolithophorid *Emiliania huxleyi* to elevated partial pressure of CO2 under nitrogen limitation., Mar. Ecol. Prog. Ser., 261, 111–122, 2003.

Shampine, L. F. and Reichelt M. W.: The MATLAB ODE Suite , SIAM Journal on Scientific Computing, 18, 1–22, 1997.

Trimborn, S., Langer, G., and Rost, B.: Effect of varying calcium concentrations and light intensities on calcification and photosynthesis in *Emiliania huxleyi*, Limnology And Oceanography, 52, 2285–2293, 2007a.

Trimborn, S., Langer, G., and Rost, B.: Effect of varying calcium concentrations and light intensities on calcification and photosynthesis in *Emiliania huxleyi*, Limnology And Oceanography, 52, 2285–2293, 2007b.

Tyrell, T. and Taylor, A.: A modelling study of *Emiliania huxleyi* in the NE Atlantic , Journal of Marine Systems, 9, 83–112, 1996.

Zeebe, R. E. and Wolf-Gladrow, D.: CO_2 in seawater: equilibrium, kinetics, isotopes, Elsevier, 2003.